HDL-Mimetic PLGA Nanoparticle To Target Atherosclerosis Plaque Macrophages

Brenda L. Sanchez-Gaytan[†,∇], **Francois Fay**[†,∇], **Mark E. Lobatto**[†,‡,∇], **Jun Tang**[†,§], **Mireille Ouimet**[‖], **YongTae Kim**[⊥], **Susanne E. M. van der Staay**[†], **Sarian M. van Rijs**[†], **Bram Priem**[†], **Liangfang Zhang**[#], **Edward A Fisher**[‖], **Kathryn J. Moore**[‖], **Robert Langer**[○], **Zahi A. Fayad**[†], and **Willem J M Mulder**[*,†,‡]

[†]Translational and Molecular Imaging Institute, New York, New York 10029, United States [§]Graduate School of Biomedical Sciences, Icahn School of Medicine at Mount Sinai, New York, New York 10029, United States [‡]Department of Vascular Medicine, Academic Medical Center, Amsterdam, 1105 AZ, The Netherlands [‖]Departments of Medicine (Cardiology) and Cell Biology, NYU School of Medicine, New York, New York 10016, United States [⊥]The George W. Woodruff School of Mechanical Engineering, Institute for Electronics and Nanotechnology, Parker H. Petit Institute for Bioengineering and Bioscience, Georgia Institute of Technology, Atlanta, Georgia 30332, United States [#]Department of NanoEngineering and Moores Cancer Center, University of California, San Diego, La Jolla, California 92093, United States [○]David H. Koch Institute for Integrative Cancer Research, Massachusetts Institute of Technology, Cambridge, Massachusetts 02139, United States
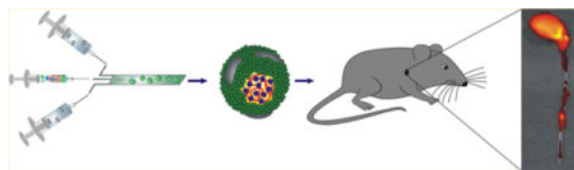
Abstract

High-density lipoprotein (HDL) is a natural nanoparticle that exhibits an intrinsic affinity for atherosclerotic plaque macrophages. Its natural targeting capability as well as the option to incorporate lipophilic payloads, e.g., imaging or therapeutic components, in both the hydrophobic core and the phospholipid corona make the HDL platform an attractive nanocarrier. To realize controlled release properties, we developed a hybrid polymer/HDL nanoparticle composed of a lipid/apolipoprotein coating that encapsulates a poly(lactic-*co*-glycolic acid) (PLGA) core. This novel HDL-like nanoparticle (PLGA–HDL) displayed natural HDL characteristics, including preferential uptake by macrophages and a good cholesterol efflux capacity, combined with a typical PLGA nanoparticle slow release profile. In vivo studies carried out with an ApoE knockout mouse model of atherosclerosis showed clear accumulation of PLGA–HDL nanoparticles in atherosclerotic plaques, which colocalized with plaque macrophages. This biomimetic platform integrates the targeting capacity of HDL biomimetic nanoparticles with the characteristic versatility of PLGA-based nanocarriers.

[*]**Corresponding Author:** Phone: 212-241-6858. Fax: 240-368-8096. Willem.Mulder@mssm.edu.
[∇]**Author Contributions**
B.L.S.-G., F.F., and M.E.L. contributed equally to this work.

INTRODUCTION

Cardiovascular disease is the pre-eminent killer in the Western world.[1] The most prominent cause of myocardial infarction and ischemic stroke is atherosclerosis, the buildup of lipids and immune cells within the arterial wall.[2] Although lipid-lowering drugs have been applied successfully for the past 25 years, novel therapeutic strategies focusing on treating vessel wall inflammation, a hallmark of atherosclerosis, have emerged in recent years.[3–5] However, the administration of anti-inflammatory drugs is associated with the occurrence of side effects, mainly systemic immunosuppression.[6] To overcome this latter issue, plaques/cells targeted treatments that have the potential to reduce side effects, while exerting direct therapeutic effects on plaque macrophages through local drug delivery, are starting to be explored in preclinical studies.[7]

Targeting atherosclerotic plaques with nanoparticles can be accomplished through several methods.[8] Our laboratory has pioneered the exploitation of a natural targeting process by mimicking the body's own nanoparticles, i.e., lipoproteins, to specifically interact with atherosclerotic plaques.[9] High-density lipoprotein (HDL), the smallest lipoprotein of the lipoprotein family (8–12 nm in diameter), consists of a core containing hydrophobic lipids surrounded by a monolayer of amphiphilic phospholipids and apolipoproteins (ApoA-I or ApoA-II).[10] In the body, HDL naturally accumulates in atherosclerotic plaques, where it interacts with ATP-binding cassette transporters A1 (ABCA1) and G1 (ABCG1) and the scavenger receptor B1 (SR-B1),[11,12] leading to cholesterol removal from lipid-laden plaque macrophages and its transport to the liver for excretion, through a process known as reverse cholesterol transport.[13] We and others have previously been able to produce biomimetic HDL labeled with a variety of contrast agents, including amphiphilic gadolinium chelates,[14] fluorophores, or diagnostic nanocrystals, including gold, iron oxide, and quantum dots.[15–17] These hybrid lipoprotein nanoparticles were successfully employed as multimodal molecular imaging agents to specifically image macrophages in atherosclerotic plaques and thus allow the noninvasive assessment of vessel wall inflammation.[18] Furthermore, the hydrophobic core of HDL can also act as a drug carrier, as we have previously incorporated statins to efficiently deliver these drugs to atherosclerotic plaques.[19] In the current study, we developed a second generation of this HDL nanoparticle platform by incorporating the polymer poly(lactic-co-glycolic acid) (PLGA) in its hydrophobic core in order to allow controlled release of drugs. PLGA is a FDA approved polymer commonly used to formulate nanocarriers that degrade over time,[20,21] ensuring a slow release of incorporated drug contents.[22,23] The rapid formation of stable sub 100 nm PLGA–HDL hybrid particles in a reproducible fashion was guaranteed by swift mixing of all different components using microfluidics technology, which we recently developed for the synthesis of lipid-polymer as well as biomimetic HDL nanoparticles.[24,25] Here, we show that our PLGA–HDL

nanoparticle platform is multifunctional and has controlled release properties and that its biological properties and ability to efficiently target plaque macrophages closely resemble that of native HDL.

RESULTS AND DISCUSSION

Nanoparticle Synthesis and Structure

Nanoparticle-based probes enable target-specific drug delivery or imaging in an elegant fashion.[8,26] Previous studies from our and other groups have shown that HDL-like particles display unique atherosclerosis-targeting features and preferentially accumulate in atherosclerotic plaque macrophages.[27] Hybrid PLGA–HDL nanoparticles were synthesized by the microfluidics technology that we recently developed and applied to formulate PEG–lipid/polymeric nanoparticles[24] as well as HDL biomimetic nanoparticles.[25] This approach enables the controlled mixing of miscible component solutions in the microfluidics device. We chose microfluidic technology to synthesize PLGA–HDL nanoparticles due to the ease of preparation, high reproducibility of different batches, and ability to mix multiple components in a single session. In this approach, phospholipids and PLGA were solubilized in a mixture of acetonitrile/ethanol and then injected in the central channel of the chip while a solution of ApoA-I in PBS was injected in the external channels (Figure 1a). Upon mixture of the different solutions, instantaneous self-assembly of the reagents occurs, leading to the formation of a hydrophobic PLGA core surrounded with a phospholipid-based coating. Simultaneously, the swift incorporation of ApoA-I into the phospholipid structure renders onestep reproducible batches of nanoparticles without the additional need for overnight incubation of ApoA-I, as was necessary in earlier HDL nanoparticle synthesis methods (Figure 1b,c). ApoA-I inclusion was found to be required to generate stable PLGA–HDL nanoparticles, as its absence resulted in large nanoparticle aggregates. Therefore, and as we have done previously,[15] a PEG–lipid coating was applied for the control nanoparticles, which results in stable formulations. The versatility of the technology permits the incorporation of a variety of therapeutic and diagnostic components both in the hydrophobic core and the phospholipid corona to generate multifunctional PLGA–HDL nanoparticles.

In nature, nascent HDL consists of discoidal nanostructures composed of a phospholipid bilayer that is encompassed by a belt of ApoA-I.[28] After several transformations that are part of normal dynamic HDL metabolism, nascent HDL gives rise to mature HDL found in the circulation.[29] These spherical particles consist of a hydrophobic core (i.e., cholesteryl esters and triglycerides) coated by a phospholipid corona in which apolipoprotein A-I is embedded. The spherical structure of the biomimetic PLGA–HDL synthesized here resembles that of mature HDL. The synthesized hybrid structure consists of a phospholipid/ApoA-I coating and a hydrophobic polymeric core that templates the spherical shape of the particle. Nanoparticle structural analysis showed that the phospholipid/ApoA-I molar ratio of PLGA–HDL was similar to the ratio of discoidal reconstituted HDL synthesized by conventional procedures (rHDL)[30] and HDL synthesized by microfluidics technology (μHDL)[25] (Table 1 and Figure S1). The purity of nanoparticle batches after synthesis and purification was assed by size exclusion chromatography (Figure S2).

Nanoparticle size was controlled by carefully modifying the flow rate of the different solutions, i.e., Reynolds number (Re).[24] The PLGA–HDL nanoparticles could be produced with a substantial hydrodynamic size range. By varying the flow rates from 10–2–10 mL/min (Re ~ 300) to 5–1–5 mL/min (Re ~ 150) (external–middle–external) in the channels, we were able to synthesize PLGA–HDL with mean sizes ranging from 88 to 156 nm, corresponding to an average of 42 000–127 000 molecules of phospholipids and 232–741 molecules of ApoA-I per particle. Zeta potential of PLGA–HDL was determined to be –7.1 mV, which is similar to the measurements obtained for rHDL and native HDL (–7.03 and –6.28 mV, respectively).

The mean size of PLGA–HDL generally decreased when flow rates were increased. Flow rates of 10 and 2 mL/min in the external and internal channels (10–2–10), respectively, resulted in nanoparticles with a mean hydrodynamic diameter of 88.1 nm and a polydispersity of 0.142 (Figure 1d,f). Flow rates of 5 mL/min in both external channels and 1 mL/min in the internal channel (5–1–5) generated nanoparticles with a mean hydrodynamic diameter of 150 nm and a polydispersity of 0.136, indicative of a small size distribution (Figure 1e,f). TEM images of nanoparticles prepared using 10 and 2 mL/min flow rates show spherical nanoparticles with sizes between 60 and 120 nm and low polydispersity (Figure 1d). Size control could also be realized by altering the lipid-to-polymer ratio. This allowed us to decrease the nanoparticle size to a diameter as small as 36 nm (Figure 1g,h). It is important to note that the unique size control in this HDL-like nanoparticle is due to the presence of a polymeric core.

PLGA–HDL nanoparticles were stable in PBS for 10 days at 4°C and 1 week at room temperature. After that time, a steady increase in size and polydispersity was observed, which is attributed to degradation of the core and subsequent aggregation of the nanoparticles. Nanoparticles incubated at 37°C showed an initial increase in size, indicative of a swollen core, followed by a subsequent slow decrease in size due to the degradation of the polymeric core (Figure S3).

Indeed, the biodegradability of PLGA and its inclusion in the polymeric nanoparticle core allows for the controlled release of its contents. PLGA-based nanoparticles have been successfully used to encapsulate hydrophobic drugs and ensure their prolonged release due to slow degradation of PLGA, which degrades into glycolic and lactic acid, byproducts of physiologic metabolic pathways.[23] The slow release properties of PLGA–HDL were tested with Nile Red, a hydrophobic dye that can, therefore, serve as a model for a drug. The release profile in PBS at 37°C confirmed slow release capabilities: around 60% of the dye was released within 24 h, with approximately 90% of the dye released after 5 days (Figure 2), whereas agent release was blunted at 4°C (Figure S4).

In addition to a HDL-like architecture, we set out to investigate if our particle mimicked certain biological functions of native HDL. Nanoparticle composition analysis showed that the apolipoprotein/phospholipid ratio hybrid of PLGA–HDL is very similar to that of HDL synthesized using other procedures. Despite differences in size and synthetic methods, we hypothesized that PLGA–HDL nanoparticles retained biological capabilities similar to those of native HDL. First, nanoparticle-induced cytotoxicity was evaluated with a 3-(4,5-

dimethylthiazol-2-yl)-2,5-diphenyltetrazolium bromide (MTT) metabolic assay using different cell lines, such as murine macrophages, hepatocytes, smooth muscle cells, and pancreatic endothelial cells. After a 24 h incubation period, no particlerelated cytotoxicity was observed in any of the studied cell lines (Figure S5). The same cell lines were incubated with rhodamine-labeled PLGA–HDL or control nanoparticles to investigate uptake or adhesion of nanoparticles. Rhodamine-labeled PEG–PLGA nanoparticles, consisting of a PLGA core surrounded by a corona made of PEGylated phospholipids with a diameter of 82 nm, were chosen as a control. PEG–PLGA NP had a similar size and composition as that of PLGA–HDL, though they lacked ApoA-I, which is largely responsible for the mimetic properties of PLGA–HDL. After a 2 h incubation period, macrophages incubated with rhodamine-labeled PLGA–HDL showed a strong fluorescent signal, indicative of a preferential interaction with PLGA–HDL (Figure 3a). The other cell types that can encounter nanoparticles within the blood circulation, such as hepatocytes in the liver, smooth muscle cells, and endothelial cells within the vessel wall (Figure 3b–d,i), did not significantly take up or adhere to nanoparticles. PEG–PLGA nanoparticles were not significantly taken up by any of the cells under the same conditions (Figure 3e–h). The preferential interaction of PLGA–HDL with macrophages was confirmed with flow cytometry analysis (Figure 3j). This behavior is typically observed with macrophages incubated with HDL[25] (Figure S6). Cultured endothelial cells (human umbilical vein endothelial cells) displayed a very similar behavior as that of other cell lines (Figure S7 and S8).

Subsequently, other bioactive properties of the PLGA–HDL nanoparticles were also tested. Competition assays were performed to determine if PLGA–HDL associated with macrophages through a similar pathway as that of native HDL.[25] To this end, PLGA–HDL and different concentrations of native HDL were coincubated with macrophages. Figure 4 shows that the interaction between macrophages and PLGA–HDL gradually decreased with increasing concentrations of native HDL, indicative of competitive inhibition.

In addition to macrophage specificity, a defining property of HDL is its cholesterol efflux capacity,[17,18,25] which is paramount to its function in reverse cholesterol transport. This efflux process has been extensively characterized for both native HDL[11,12] and HDL-like nanoparticles[17] and has been shown to primarily involve the interaction of ApoA-I with specific efflux membrane proteins such as Scavenger receptor class B type I (SRB1) and the ATP-binding cassette transporters A1 and G1 (ABC1, ABG1). Cholesterol efflux assays were performed in human macrophage-like THP-1 cells, murine bone marrow-derived macrophages, and the murine macrophage cell line J774A.1 (Figure S9) and were compared to native or microfluidics reconstituted HDL using bovine serum albumin as control. Significant cholesterol efflux capabilities to PLGA–HDL were observed in all cell lines. Figure 5 shows the cholesterol efflux results for THP-1 human macrophages. A considerable amount of cellular cholesterol efflux to PLGA–HDL was observed, which was lower in most cell lines than what was observed for native HDL. This is something we attribute to the PLGA core, which reduces the available space for cholesterol inclusion. Still, the behavior displayed by PLGA–HDL strongly resembles that of native or reconstituted HDLs, suggesting that the same pathways responsible for the HDL-mediated cholesterol efflux are involved in the PLGA–HDL-mediated cholesterol efflux. Together, the selective uptake of

PLGA–HDL by macrophages and the ability of PLGA–HDL to serve as a cholesterol acceptor during cholesterol efflux assays confirmed the biomimetic HDL-like capabilities of PLGA–HDL.

PLGA–HDL Targets Macrophages in Atherosclerotic Lesions of Apolipoprotein E Knockout (ApoE-KO) Mice

Ex vivo studies involved first the determination of blood half-life and biodistribution of the DMPC/MHPC PLGA–HDL nanoparticles. The half-life was found to be 12.8 h (Figure S10). Biodistribution analyses on heart, aorta, spleen, liver, kidney, brain, and muscle tissues were done by NIRF imaging and revealed, similar to other platforms,[31–33] that the PLGA–HDL nanoparticles were predominantly cleared by the liver and spleen (Figure S11).

We proceeded to evaluate the preferential and specific targeting of macrophages by PLGA–HDL in ApoE-KO mice, a mouse model of atherosclerosis. To this end, we synthesized PLGA–HDL labeled with the fluorescent dye DiR to facilitate imaging with a variety of optical techniques, including NIRF imaging, fluorescence microscopy, and flow cytometry. PLGA–HDL or saline solution was administered by tail vein injections. Twenty-four hours later, aortas and aortic roots of the mice were harvested and imaged with a NIRF system (n = 3 for both groups). NIRF imaging of excised aortas (Figure 6a,b) revealed heterogeneous uptake of PLGA–HDL along the aorta and the aortic root, locations where atherosclerotic lesions are typically present in this disease model. To further investigate nanoparticle uptake at a cellular level, aortic roots were sectioned, fixed, stained, then imaged by fluorescence microscopy. A fluorescence microscopy image (Figure 6c, left) revealed colocalization of PLGA–HDL with a staining for macrophages (CD68^{+}), indicative of preferential interaction. The remaining aortas were subsequently digested to perform flow cytometry to validate these results. Flow cytometry data further corroborated previous findings, as PLGA–HDL was shown to predominantly associate with macrophages within the aortas (Figure 6c, right). This preferential uptake is key for future anti-inflammatory therapies in atherosclerosis using this PLGA–HDL platform since inflammatory macrophages contribute to atherosclerosis aggravation and may degrade the extracellular matrix by secreting destructive proteases.[34] These data are in line with previous findings by us and others showing that HDL-type particles target atherosclerotic plaques and preferentially accumulate in plaque macrophages.[27]

CONCLUSIONS

Hybrid Polymer–HDL nanoparticles with a PLGA core and a coating composed of lipids and apolipoprotein A-I were synthesized using microfluidic technology. Due to its complex design, the nanoparticle core is suitable for delivery of drugs in a controlled manner, while the coating provides the nanoparticle with biological capabilities similar to those found in native HDL (e.g., macrophage targeting and cholesterol efflux capacities). Importantly, results show that PLGA–HDL nanoparticles preferentially associate with macrophages and monocytes within the aorta. Furthermore, the versatility of the approach allows the incorporation of functional lipids to render multifunctional nanoparticles with diagnostic, therapeutic, and atherosclerosis-targeting properties.

MATERIALS AND METHODS

Materials

Nile Red, poly(D,L-lactide-*co*-glycolide) (PLGA 50:50; MW 30 000–60 000), acetonitrile (ACN), ethanol, fetal bovine serum, hyaluronidase, and DNase I were purchased from Sigma-Aldrich. Phosphate buffered saline solutions (PBS) were purchased from Fisher Scientific. 1-Stearoyl-2-hydroxy-*sn*-glycero-3-phosphocholine (SHPC), 1,2-distearoyl-*sn*-glycero-3-phosphocholine (DSPC), 1,2-dimyristoyl-*sn*-glycero-3-phosphocholine (DMPC), 1-myristoyl-2-hydroxy-*sn*-glycero-3-phosphocholine (MHPC), 1,2-distearoyl-*sn*-glycero-3-phosphoethanolamine-*N*-[methoxy(polyethylene glycol)-2000] (ammonium salt) (DSPE-PEG2000), and 1,2-dimyristoyl-*sn*-glycero-3-phosphoethanolamine-*N*-(lissamine rhodamine B sulfonyl)(ammonium salt) (rhodamine-DMPE) were purchased from Avanti Polar Lipids, Inc. Lipophilic tracers DiO and DiR were purchased from Life Technologies. Apolipoprotein A-I (ApoA-I) of 95% purity was kindly provided by CSL Behring. Murine hepatoma cells Hepa1c1c7 (CRL-2026), murine aorta/smooth muscle cells MOVAS (CRL-2797), murine sarcoma macrophage cells J774A.1 (TIB-67), murine pancreas/islet of Langerhans endothelium MS1MILE SVEN 1 (CRL-2279), and human umbilical vein endothelial cells (HUVEC, CRL-1730) were purchased from ATCC. Streptomycin/penicillin was purchased from Cellgro Mediatech. DAPI was purchased from Vector Labs. Anti-CD68 antibodies were purchased from Serotec Laboratories. Native HDL from human plasma was purchased from Biomedical Technologies (BT-914).

Synthesis of PLGA–HDL, PEG–PLGA, and HDL Nanoparticles

Synthesis of PLGA–HDL—Two lipid combinations were tested: 1-stearoyl-2-hydroxy-*sn*-glycero-3-phosphocholine (SHPC)/1,2-distearoyl-*sn*-glycero-3-phosphocholine (DSPC) and 1,2-dimyristoyl-*sn*-glycero-3-phosphocholine (DMPC)/1-myristoyl-2-hydroxy-*sn*-glycero-3-phosphocholine (MHPC). For a ~80 nm size nanoparticle, a solution containing 0.5 mL of a PLGA solution in acetonitrile (100 mg/mL), 5 mL of a 1:1 molar ratio of SHPC/DSPC or a 3:1 DMPC/MHPC solution in ethanol (1 mg/mL), and 14.5 mL of acetonitrile was prepared. To formulate the nanoparticles, we used the microfluidics technology that we developed previously.[24] The aforementioned solution was injected in the middle channel of the microfluidic chip at a rate of 10 mL/min, while a solution of ApoA-I (0.01 mg/mL in 1× PBS) was injected in the outer channels at a rate of 2 mL/min. The product was collected, washed with PBS, and concentrated with centrifugal concentration devices (100 000 MWCO) to remove acetonitrile, ethanol, and lipid-free ApoA-I. One milligram of Nile Red was included in the PLGA–phospholipid solution to measure its release profile as a model for a therapeutic payload. For the in vitro cell uptake studies, 2% phospholipid by weight was substituted with rhodamine-DMPE. Alternatively, for the in vivo studies, 0.05 mg of DiR or DiO was included. Smaller nanoparticle sizes are obtained by lowering the PLGA–to-lipid ratio (see table in Figure 1). The data shown in the Results and Discussion was generated with DSPC/SHPC-coated PLGA–HDL nanoparticles, unless otherwise indicated. Data on the DMPC/MHPC-based formulation is presented in Figure S1.

Synthesis of PEG–PLGA Nanoparticles—Control PEG–PLGA nanoparticles (PEG–PLGA NP) were synthesized by injecting a mixture of 0.5 mL of a PLGA solution in

acetonitrile (100 mg/mL), 5 mL of a 7:3 molar ratio of DSPC/DSPE-PEG2000 solution in ethanol (2 mg/mL), and 14.5 mL of acetonitrile in the middle channel at a flow rate of 1 mL/min. Deionized water was injected in the exterior channels at a rate of 5 mL/min. For the cell studies, 1% phospholipid by weight was substituted with rhodamine-DMPE. The product was collected, washed with water, and concentrated with centrifugal concentration devices (100 000 MWCO).

Synthesis of μHDL—Reconstituted HDL (μHDL) was synthesized using the microfluidic chip, as recently reported.[25] A solution of DMPC in ethanol (2 mg/mL) was injected in the middle channel of the microfluidic device at a rate of 1 mL/ min, and a solution of ApoA-I in PBS (0.2 mg/mL) was added in the external channels at a rate of 5 mL/min. The product was collected, washed with PBS, and concentrated with centrifugal concentration devices (10 000 MWCO).

Synthesis of rHDL—Reconstituted HDL (rHDL) was synthesized by a lipids hydration method. Briefly, a solution of DMPC in chloroform (5 mg/mL) was placed in a glass vial and dried to form a thin film using a vacuum-based desiccator. Once completely dried, a solution of ApoA-I in 5 mL of PBS was added for a final ratio of lipid/ApoA-I of 2.5 by mass. The mixture was incubated for 3 h at 37°C until a homogeneous solution was formed. The solution was then placed under tip sonication for 1 h under an ice bath. Aggregates were removed by centrifugation at 2000 rpm for 10 min. For fluorescence microscopy studies, 1% of the lipid weight was substituted with rhodamine-DMPE.

Determination of Nanoparticle Diameters by Dynamic Light Scattering (DLS)

PLGA–HDL nanoparticles were analyzed by DLS (Brookhaven Instruments Coorporation). In short, 10 μL of each sample was suspended in 490 μL of PBS and subsequently measured 10 times, from which the mean diameter and polydispersity were calculated.

Determination of Nanoparticle Charge by Zeta Potential

PLGA–HDL nanoparticle charge was measured at 37°C using a zeta potential analyzer (Brookhaven Instruments Coorporation). Each sample was measured five times, and the average was calculated.

Transmission Electron Microscopy (TEM) Characterization

The nanoparticle's original buffer solution was exchanged with acetate buffer (0.125 M ammonium acetate, 2.6 mM ammonium carbonate, and 0.26 mM tetrasodium ethylenediaminetetraacetate (EDTA) at pH 7.4) using centrifugal concentration devices (MWCO 100 000). A 10 μL solution of nanoparticles in acetate buffer was mixed with 10 μL of a 2% phosphotungstic acid solution to be negatively stained and then cast on a 100 mesh Formvar coated nickel grid (Electron Microscopy Sciences). The TEM images were acquired using a Hitachi 7650 TEM microscope operated at 80 kV coupled to a Scientific Instruments and Applications (SIA) digital camera controlled by Maxim CCD software.

Drug Release Profile

In order to evaluate nanoparticle drug release, Nile Red-loaded PLGA–HDL was synthesized as described above, and the sample was placed in several 0.5 mL dialysis cassettes with a 2000 MWCO membrane. Nile Red release was measured in an aqueous phosphate buffer at 37°C under constant stirring. At each time point, the sample was removed from the cassette, dried, and extracted before the fluorescence was analyzed with a microplate reader.

Phosphate and ApoA-I Determinations

The amount of phospholipids in the nanoparticles was determined by a molybdate reaction following the Rouser method;[35] the ApoA-I concentration was determined following the Markwell method.[36]

Cell Propagation

Murine sarcoma macrophage cells J774A.1 (TIB-67), murine aorta/smooth muscle cells MOVAS (CRL-2797), murine pancreas/islet of Langerhans endothelium MS1MILE SVEN 1 (CRL-2279), and human umbilical vein endothelial cells HUVEC (CRL-1730) were propagated in a Dulbecco's modified Eagle's medium supplemented with 1% streptomycin/penicillin and 10% fetal bovine serum. Murine hepatoma cells Hepa1c1c7 (CRL-2026) were propagated in alpha minimum essential medium without nucleosides supplemented with 1% streptomycin/penicillin and 10% fetal bovine serum. Before experiments, cells were detached, washed in PBS, and counted. Defined numbers of cells were then seeded and left overnight to adhere.

Macrophage-Targeting Assay

The rhodamine content of PLGA–HDL and PEG–PLGA NP was determined in a fluorescence microplate reader, and the concentrations of the nanoparticle solutions were adjusted so that they had the same rhodamine emission intensity. Cells were seeded on black opaque 96-well plates and allowed to adhere overnight. The cell media was then refreshed, and cells were incubated with rhodamine-labeled PLGA–HDL or the corresponding amount of PEG–PLGA NP. Cells were subsequently washed with PBS to discard nonbound/internalized particles. Fluorescence of bound/internalized nanoparticles was measured using a fluorescent plate reader with excitation at 550 nm and emission at 590 nm. For competition–inhibition experiments, J774A.1 macrophages were coincubated with a fixed concentration of rhodamine-labeled PLGA–HDL corresponding to an ApoA-I concentration of 22.4 μg/mL and increasing amounts of native human HDL extracted from serum from 22.4 to 224 μg/mL with respect to protein concentration.

Fluorescence Microscopy

Cells were seeded on microscope chamber slides (LAB-TEK Nunc) and allowed to adhere overnight. The number of cells seeded was as follows: 16 500 for MS1, 100 000 for J774A.1, 13 200 for MOVAS, 33 000 HEPA, and 16 500 for HUVEC. The cell media was subsequently refreshed, and cells were incubated with rhodamine-labeled PLGA–HDL at a PLGA concentration of 0.31 mg/mL, which corresponded with a 100 μM rhodamine

concentration or the corresponding amount of PEG–PLGA NP for 2 h. After incubation, slides were washed three times with PBS, and cells were fixed with 4% paraformaldehyde for 30 min at 37°C. Slides were then washed again three times with PBS and mounted with mounting media containing DAPI. Fluorescence microscopy was performed on a Zeiss Axioplan 2 microscope.

Cholesterol Efflux Assay

THP-1 cells were differentiated to macrophages using 100 nM phorbol 12-myristate 13-acetate (PMA) for 74 h and subsequently incubated with media containing 0.5 μCi/ml [^{3}H]-cholesterol and acLDL (50 μg/mL or 20 μg/mL) for 24 h. Cells were washed twice with PBS and equilibrated for 24 h in media containing 2 mg/mL fatty acidfree albumin. Efflux to HDL or PLGA–HDL was carried out for 8 h. Cell media was removed, and the cells were lysed in 0.1 M NaOH solution. The [^{3}H]-cholesterol content of media and cell lysates was measured with liquid scintillation counting, and efflux is expressed as a percentage of [^{3}H]-cholesterol in medium/([^{3}H]-cholesterol in medium + [^{3}H]-cholesterol in cells) $\times$ 100%.

In Vitro Flow Cytometry

Murine sarcoma macrophage cells J774A.1 were seeded at 300 000 cells per well into 6-well plates and allowed to adhere overnight. The cell media was then refreshed, and cells were incubated with rhodamine-labeled PLGA–HDL or the corresponding amount of PEG–PLGA NP. After incubation, cells were washed three times with PBS, detached, washed again, and suspended in PBS. Cell fluorescence was then measured using a LSR II flow cytometer (BD Bioscience, San Jose, CA), and 10 000 events were measured. Intact cells were first gated based on their light scatter properties and their fluorescence (532/575 nm excitation and emission, respectively). Flow cytometry data was analyzed using FlowJO software (Tree star, Ashland OR).

Cell Viability

Cells were seeded in 96-well plates and allowed to adhere overnight. The cell media was then refreshed, and cells were incubated with PLGA–HDL or the corresponding amount of PEG–PLGA NP for 24 h. Cell viability was assessed by the 3-(4,5-dimethylthiazol-2-yl)-2,5-diphenyltetrazolium bromide (MTT) colorimetric assay. MTT solution (20 μL of 5 mg/mL in PBS) was added to each well, and the plates were incubated for 2 h to allow the formation of formazan crystals. The medium solution was then removed, 100 mL of dimethyl sulfoxide was added, and optical densities were determined at 570 nm in a microplate reader (Spectra Max M5, Molecular Devices). Cell survival percentages were calculated from absorbance ratios when compared to untreated control cells.

Animal Model

Five week old male ApoE knockout mice (B6.129P2-Apoe[tm1Unc/j]) were obtained from The Jackson Laboratory and fed a high cholesterol diet (Research Diets Inc.), containing 20.3% fat, 22.9% protein, 45.7% carbohydrate, and 0.2% cholesterol, for 18 weeks. Mice were injected by tail vein; three mice received a single injection consisting of 0.2 mL of PLGA–HDL (~10 mg/mL; ~40 nm in diameter), and three were injected the equivalent volume of

saline as a control (n = 6 total). For nanoparticle circulation half-life, blood was drawn retro-orbitally at 5 and 30 min and 1, 6, and 24 h. Animals were sacrificed 24 h after injection, and liver, spleen, lungs, brain muscle, and aorta, including the root, were harvested under a microscope after they were perfused with PBS. All animal experiments were approved by the Institutional Animal Care and Use Committee at the Icahn School of Medicine at Mount Sinai.

Ex Vivo Near-Infrared Fluorescence (NIRF) Imaging

NIRF imaging of DiR was performed on a Xenogen IVIS-200 optical imaging system. The excitation and emission filters were set to 745 and 820 nm, with an exposure time of 4 s, binning at 4, and a field of view of 12.2 cm. The data were analyzed by carefully tracing the complete aorta, including the aortic root, and comparing the total radiant efficiency for both groups with Living Image 4.0 (PerkinElmer).

Fluorescence Microscopy of Aortic Roots

Aortic roots were embedded in OCT blocks and placed in a −80°C freezer. Five micrometer thick sections of the aortic root were cut on a cryotome by an experienced technician. Sections were stained with rat anti-mouse anti-CD68 antibodies (Serotec laboratories) and Cy3–conjugated anti-rat antibodies (Jackson ImmunoResearch) to detect macrophages in the aortic root. Fluorescence microscopy was performed on a Zeiss Axioplan 2 microscope.

Flow Cytometry of Digested Aortas

Harvested aortas were first cut into small pieces and then enzymatically digested by incubating them for 90 min in a Hank's balanced salt solution containing 4 U/mL liberase LH (Roche), 0.1 mg/mL DNase I, and 60 U/mL hyaluronidase at 37°C. The cell suspension was then passed through a 70 μm filter and incubated for 30 min at 4°C with macrophage/monocytespecific antibody cocktails. After washing, cell fluorescence was analyzed with a LSR II flow cytometer (BD Biosciences). The following panel of antibodies was used: Lin1 (CD90 (clone 53–2.1), CD45R (clone RA3–6B2), CD49b (clone DX5), NK1.1 (clone PK136), ly-6G (clone IA8), Ter119-e450 (clone TER-119)), CD11c (clone HL3), CD11b (clone M1/70), ly-6c (clone AL-21), and F4/80 (clone BM8). Macrophages were identified as Lin1$^-$ CD11b^{high} F4/80^{high}, whereas monocytes were identified as Lin1$^-$ CD11b^{high} F4/80$^-$ CD11C$^-$ ly-6c$^{low/high}$. Flow cytometry data was analyzed using FlowJO software (Tree Star, Ashland, OR).

Supplementary Material

Refer to Web version on PubMed Central for supplementary material.

Acknowledgments

References

1. Mitka M. New basic care goals seek to rein in global rise in cardiovascular disease. JAMA, J Am Med Assoc. 2012; 308:1725–1726.

2. Libby P. Inflammation in atherosclerosis. Nature. 2002; 420:868–874. [PubMed: 12490960]

3. Libby P, Ridker PM, Hansson GK. Progress and challenges in translating the biology of atherosclerosis. Nature. 2011; 473:317–325. [PubMed: 21593864]

4. Majmudar MD, Keliher EJ, Heidt T, Leuschner F, Truelove J, Sena BF, Gorbatov R, Iwamoto Y, Dutta P, Wojtkiewicz G, Courties G, Sebas M, Borodovsky A, Fitzgerald K, Nolte MW, Dickneite G, Chen JW, Anderson DG, Swirski FK, Weissleder R, Nahrendorf M. Monocyte-directed RNAi targeting CCR2 improves infarct healing in atherosclerosisprone mice. Circulation. 2013; 127:2038–2046. [PubMed: 23616627]

5. Charo IF, Taub R. Anti-inflammatory therapeutics for the treatment of atherosclerosis. Nat Rev Drug Discovery. 2011; 10:365–376.

6. Barnes PJ. Glucocorticosteroids: current and future directions. Br J Pharmacol. 2011; 163:29–43. [PubMed: 21198556]

7. Lobatto ME, Fayad ZA, Silvera S, Vucic E, Calcagno C, Mani V, Dickson SD, Nicolay K, Banciu M, Schiffelers RM, Metselaar JM, van Bloois L, Wu HS, Fallon JT, Rudd JH, Fuster V, Fisher EA, Storm G, Mulder WJM. Multimodal clinical imaging to longitudinally assess a nanomedical anti-inflammatory treatment in experimental atherosclerosis. Mol Pharmaceutics. 2010; 7:2020–2029.

8. Lobatto ME, Fuster V, Fayad ZA, Mulder WJM. Perspectives and opportunities for nanomedicine in the management of atherosclerosis. Nat Rev Drug Discovery. 2011; 10:835–852.

9. Cormode DP, Jarzyna PA, Mulder WJM, Fayad ZA. Modified natural nanoparticles as contrast agents for medical imaging. Adv Drug Delivery Rev. 2010; 62:329–338.

10. Gordon SM, Deng J, Lu LJ, Davidson WS. Proteomic characterization of human plasma high density lipoprotein fractionated by gel filtration chromatography. J Proteome Res. 2010; 9:5239–5249. [PubMed: 20718489]

11. Wang N, Lan D, Chen W, Matsuura F, Tall AR. ATP-binding cassette transporters G1 and G4 mediate cellular cholesterol efflux to high-density lipoproteins. Proc Natl Acad Sci USA. 2004; 101:9774–9779. [PubMed: 15210959]

12. Duong M, Collins HL, Jin W, Zanotti I, Favari E, Rothblat GH. Relative contributions of ABCA1 and SR-BI to cholesterol efflux to serum from fibroblasts and macrophages. Arterioscler, Thromb, Vasc Biol. 2006; 26:541–547. [PubMed: 16410457]

13. Fisher EA, Feig JE, Hewing B, Hazen SL, Smith JD. High-density lipoprotein function, dysfunction, and reverse cholesterol transport. Arterioscler, Thromb, Vasc Biol. 2012; 32:2813–2820. [PubMed: 23152494]

14. Frias JC, Ma Y, Williams KJ, Fayad ZA, Fisher EA. Properties of a versatile nanoparticle platform contrast agent to image and characterize atherosclerotic plaques by magnetic resonance imaging. Nano Lett. 2006; 6:2220–2224. [PubMed: 17034087]

15. Cormode DP, Skajaa T, van Schooneveld MM, Koole R, Jarzyna P, Lobatto ME, Calcagno C, Barazza A, Gordon RE, Zanzonico P, Fisher EA, Fayad ZA, Mulder WJM. Nanocrystal core high-density lipoproteins: a multimodality contrast agent platform. Nano Lett. 2008; 8:3715–3723. [PubMed: 18939808]

16. McMahon KM, Mutharasan RK, Tripathy S, Veliceasa D, Bobeica M, Shumaker DK, Luthi AJ, Helfand BT, Ardehali H, Mirkin CA, Volpert O, Thaxton CS. Biomimetic high density lipoprotein nanoparticles for nucleic acid delivery. Nano Lett. 2011; 11:1208–1214. [PubMed: 21319839]

17. Luthi AJ, Zhang H, Kim D, Giljohann DA, Mirkin CA, Thaxton CS. Tailoring of biomimetic high-density lipoprotein nanostructures changes cholesterol binding and efflux. ACS Nano. 2012; 6:276–285. [PubMed: 22117189]

18. Skajaa T, Cormode DP, Falk E, Mulder WJM, Fisher EA, Fayad ZA. High-density lipoprotein-based contrast agents for multimodal imaging of atherosclerosis. Arterioscler, Thromb, Vasc Biol. 2010; 30:169–176. [PubMed: 19815819]

19. Tang J, Duivenvoorden R, Izquierdo-Garcia D, Cormode DP, Stroes ES, Lobatto ME, Kuan EL, Randolph GL, Fuster V, Fisher EA, Mulder WJM. A statin-loaded nanotherapy increases anti-inflammatory effects of statin on atherosclerosis. Circulation. 2011:A9601.

20. Makadia HK, Siegel SJ. Poly lactic-co-glycolic acid (PLGA) as biodegradable controlled drug delivery carrier. Polymers. 2011; 3:1377–1397. [PubMed: 22577513]

21. Cheng J, Teply BA, Sherifi I, Sung J, Luther G, Gu FX, Levy-Nissenbaum E, Radovic-Moreno AF, Langer R, Farokhzad OC. Formulation of functionalized PLGA–PEG nanoparticles for in vivo targeted drug delivery. Biomaterials. 2007; 28:869–876. [PubMed: 17055572]

22. Dhar S, Gu FX, Langer R, Farokhzad OC, Lippard SJ. Targeted delivery of cisplatin to prostate cancer cells by aptamer functionalized Pt(IV) prodrug-PLGA–PEG nanoparticles. Proc Natl Acad Sci USA. 2008; 105:17356–17361. [PubMed: 18978032]

23. Kamaly N, Xiao Z, Valencia PM, Radovic-Moreno AF, Farokhzad OC. Targeted polymeric therapeutic nanoparticles: design, development and clinical translation. Chem Soc Rev. 2012; 41:2971–3010. [PubMed: 22388185]

24. Kim Y, Lee Chung B, Ma M, Mulder WJM, Fayad ZA, Farokhzad OC, Langer R. Mass production and size control of lipid polymer hybrid nanoparticles through controlled microvortices. Nano Lett. 2012; 12:3587–3591. [PubMed: 22716029]

25. Kim Y, Fay F, Cormode DP, Sanchez-Gaytan BL, Tang J, Hennessy EJ, Ma M, Moore K, Farokhzad OC, Fisher EA, Mulder WJM, Langer R, Fayad ZA. Single step reconstitution of multifunctional high-density lipoprotein-derived nanomaterials using microfluidics. ACS Nano. 2013; 7:9975–9983. [PubMed: 24079940]

26. Farokhzad OC, Langer R. Nanomedicine: developing smarter therapeutic and diagnostic modalities. Adv Drug Delivery Rev. 2006; 58:1456–1459.

27. Frias JC, Williams KJ, Fisher EA, Fayad ZA. Recombinant HDL-like nanoparticles: a specific contrast agent for MRI of atherosclerotic plaques. J Am Chem Soc. 2004; 126:16316–16317. [PubMed: 15600321]

28. Lund-Katz S, Liu L, Thuahnai ST, Philips MC. High density lipiprotein structure. Front Biosci. 2003; 8:d1044–1054. [PubMed: 12700101]

29. Shih AY, Sligar SG, Schulten K. Maturation of high-density lipoproteins. J R Soc, Interface. 2009; 6:863–871. [PubMed: 19570799]

30. Jonas A. Reconstitution of high-density lipoproteins. Methods Enzymol. 1986; 128:553–582. [PubMed: 3724523]

31. Duivenvoorden, Rl; Tang, J.; Cormode, DP.; Mieszawska, AJ.; Izquierdo-Garcia, D.; Ozcan, C.; Otten, MJ.; Zaidi, N.; Lobatto, ME.; van Rijs, SM.; Priem, B.; Kuan, EL.; Martel, C.; Hewing, B.; Sager, H.; Nahrendorf, M.; Randolph, GJ.; Stroes, ESG.; Fuster, V.; Fisher, EA.; Fayad, ZA.; Mulder, WJM. A statin-loaded reconstituted high-density lipoprotein nanoparticle inhibits atherosclerotic plaque inflammation. Nat Commun. 2014; 5:3065. [PubMed: 24445279]

32. Hu CMJ, Zhang L, Aryal S, Cheung C, Fang RH, Zhang L. Erythrocyte membrane-camouflaged polymeric nanoparticles as a biomimetic delivery platform. Proc Natl Acad Sci USA. 2011; 108:10980–10985. [PubMed: 21690347]

33. Lee MJE, Veiseh O, Bhattarai N, Sun C, Hansen SJ, Ditzler S, Knoblaugh S, Lee D, Ellenbogen R, Zhang M, Olson JM. Rapid pharmacokinetic and biodistribution studies using cholorotoxin-conjugated iron oxide nanoparticles: a novel nonradioactive method. PLoS One. 2010; 5:e9536. [PubMed: 20209054]

34. Swirski FK, Nahrendorf M. Leukocyte behavior in atherosclerosis, myocardial infarction, and heart failure. Science. 2013; 339:161–166. [PubMed: 23307733]

35. Rouser G, Fleischer S, Yamamoto A. Two dimensional thin layer chromatographic separation of polar lipids and determination of phospholipids by phosphorus analysis of spots. Lipids. 1970; 5:494–496. [PubMed: 5483450]

36. Markwell MAK, Haas SM, Bieber LL, Tolbert NE. A modification of the Lowry procedure to simplify protein determination in membrane and lipoprotein samples. Anal Biochem. 1978; 87:206–210. [PubMed: 98070]
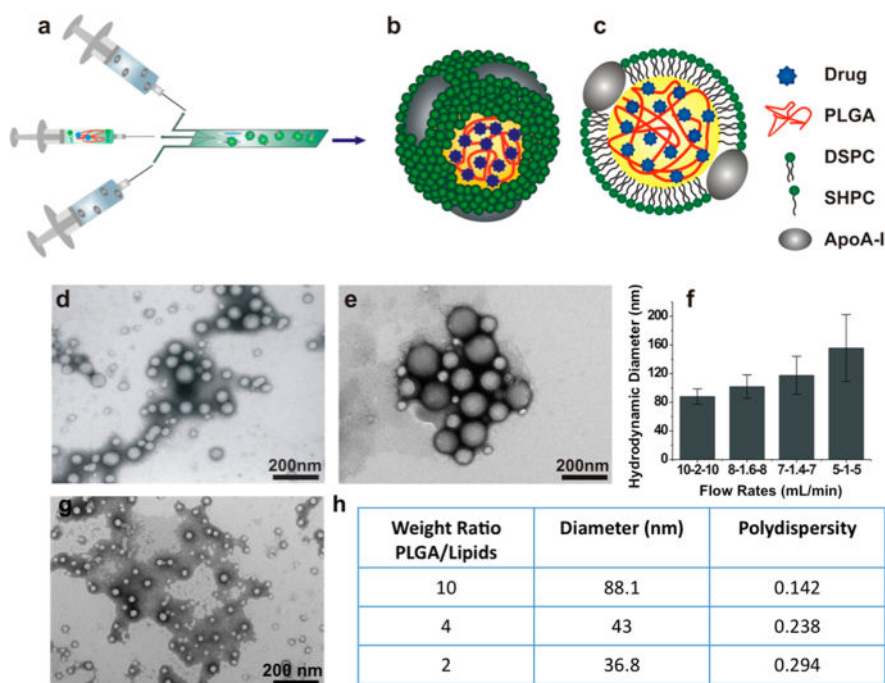
Figure 1.
Schematic depiction of the synthesis of PLGA–HDL by microfluidic technology (a). 3D and 2D schematics of the nanoparticle structure (b, c). Transmission electron micrograph of PLGA–HDL nanoparticles at flow rates of 10–2–10 mL/min (d) and 5–1–5 mL/min (e). Graph showing the size dependence of PLGA–HDL nanoparticles at various flow rates. Samples for each flow rate were made in triplicate ($n = 3$), with 10 DLS measurements each. From left to right: 10–2–10, 8–1.6–8, 7–1.4–7, and 5–1–5 flow rates (external–entral–external) (f). Transmission electron micrograph of PLGA–HDL nanoparticles at PLGA/lipid ratio of 4 (g). Table showing the effect of polymer/lipid ratio on nanoparticle size (h).
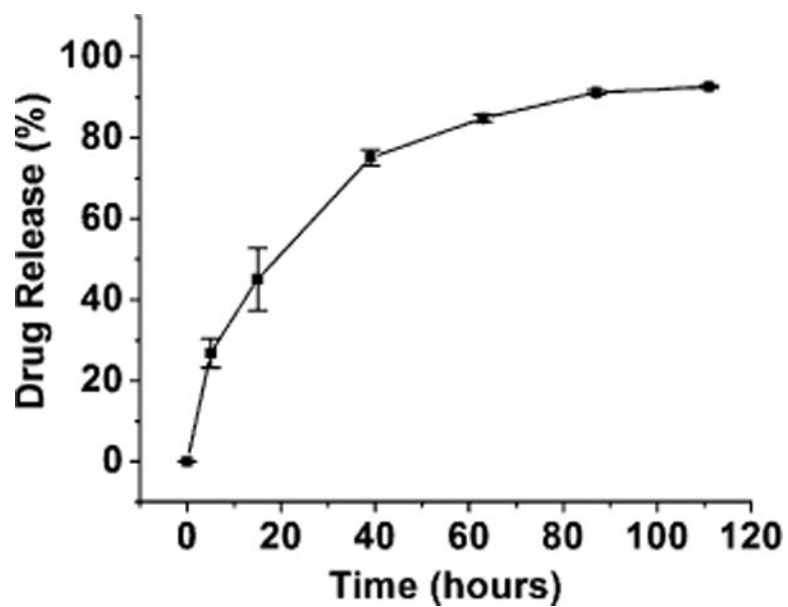
Figure 2.
Release profile of Nile Red-containing PLGA–HDL nanoparticles at 37°C in PBS; $n = 3$.
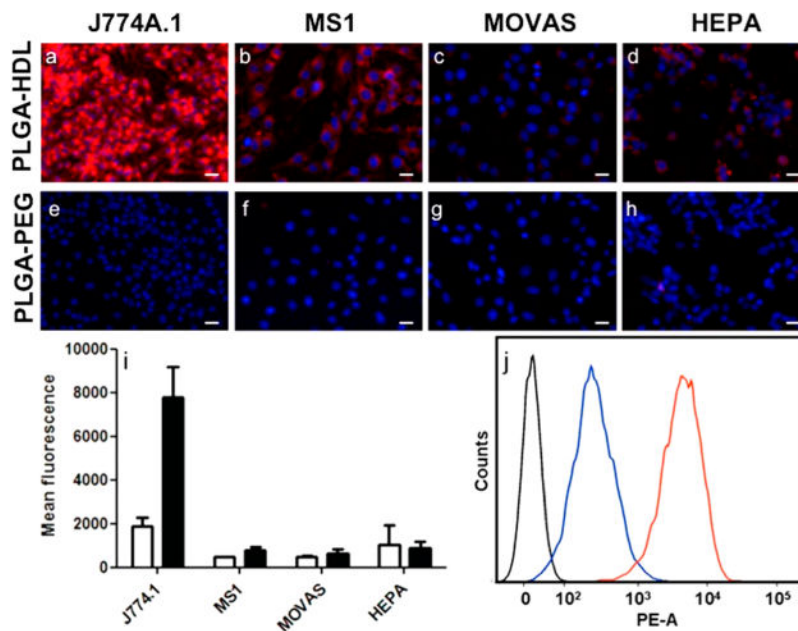
Figure 3.
Fluorescence microscopy images of DAPI-stained macrophages (a, e), pancreatic endothelial cells (b, f), smooth muscle cells (c, g), and hepatocytes (d, h) incubated with rhodamine-labeled PLGA–HDL nanoparticles (a–d) and rhodamine-labeled control PEG–PLGA nanoparticles (e–h). The scale bar is 25 μm. (i) Mean fluorescence of macrophages, pancreatic endothelial cells, smooth muscle cells, and hepatocytes incubated with PEG–PLGA NP (white) and PLGA–HDL (black). (j) Flow cytometry of macrophages incubated with PLGA–HDL (red), PEG–PLGA NP (blue) nanoparticles, and PBS (black) for 2 h at 37°C.
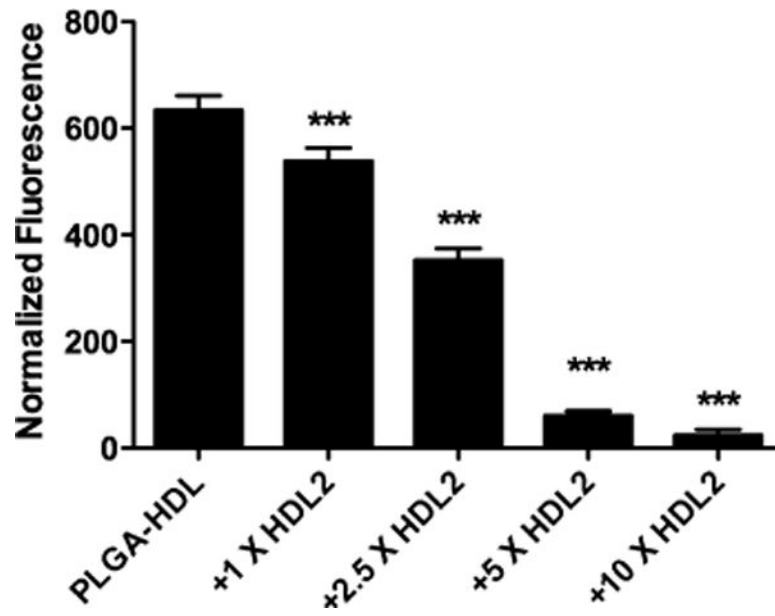
Figure 4.
Competition assay shows a decrease in PLGA–HDL uptake upon addition of increasing amounts of native HDL. Amount of HDL added from left to right: 0, 1, 2.5, 5, and 10 times the amount of PLGA–HDL.
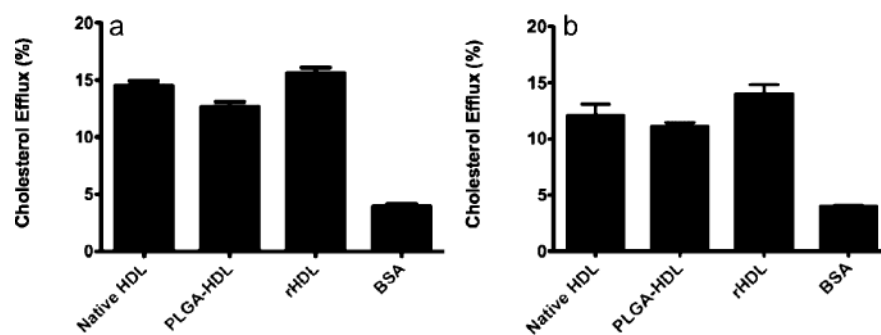
Figure 5.
Cholesterol efflux assay of native-HDL, PLGA–HDL, and microfluidic-synthesized HDL on human macrophage-like THP-1 cells at (a) 50 μg/mL and (b) 20 μg/mL.
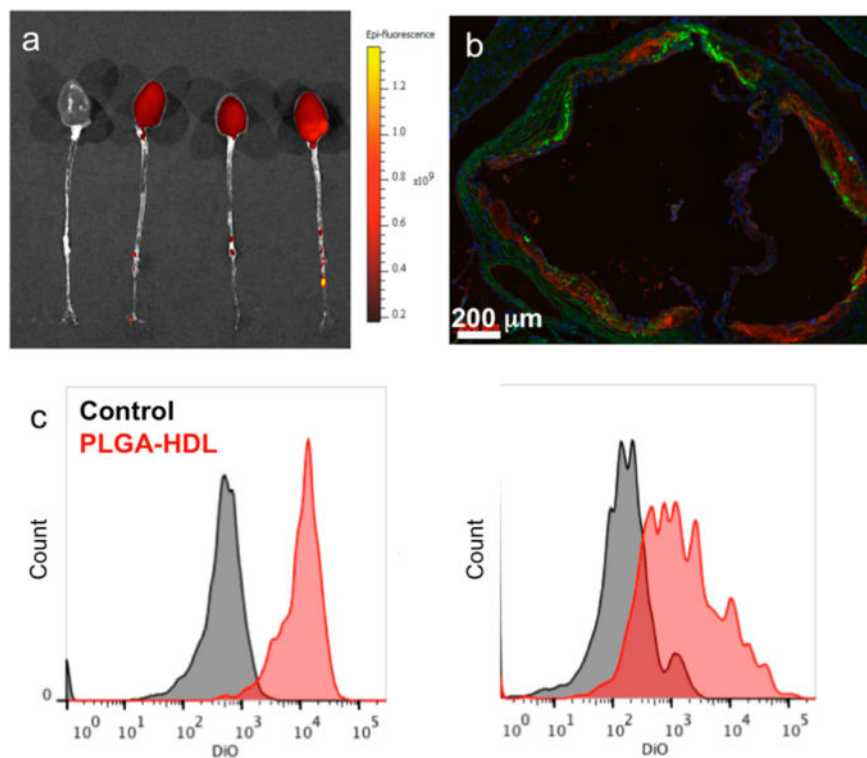
Figure 6.
PLGA–HDL nanoparticles target atherosclerotic plaques. (a) Fluorescence imaging of excised aortas of ApoE-KO mice injected with placebo or PLGA–HDL nanoparticles. Uptake can be seen throughout the thoracic and abdominal aorta as well as in the aortic root of the PLGA–HDL injected mouse. (b) A stitched 20× fluorescence microscopy image is shown of the aortic root (scale bar, 200 μm): red signifies a stain for CD68, green, PLGA–HDL, and blue, cell nuclei (DAPI). (c) Fluorescent activated cell sorting of digested aortas injected with PLGA–HDL; the label DiR is mainly associated with monocytes (left) and macrophages in the aorta (right).

Table 1

Phospholipid-to-ApoA-I Ratio of Different HDL Nanoparticles

sample	phospholipids/ApoA-I (moles)
PLGA–HDL	172
μHDL	112
rHDL	128